ELSEVIER

Biophysical Chemistry 71 (1998) 235–243

Biophysical Chemistry

# Actinic light and pH effect on the proton pumping of bacteriorhodopsin

Zs. Ablonczy, Viet Hien Ha, E. Papp *

*Department of Atomic Physics, Eötvös University, Puskin u. 5–7, Budapest H-1088, Hungary*

Received 17 November 1997; accepted 8 January 1998

**Abstract**

The actinic light effect on the bacteriorhodopsin (BR) photocycle kinetics led to the assumption of a cooperative interaction between the photocycling BR molecules. In this paper we report the results of the actinic light effect and pH on the proton release and uptake kinetics. An electrical method is applied to detect proton release and uptake during the photocycle [E. Papp, G. Fricsovszky, J. Photochem. Photobiol. B: Biol. 5 (1990) 321]. The BR photocycle kinetics was also studied by absorption kinetics measurements at 410 nm and the data were analyzed by the local analysis of the M state kinetics [E. Papp, V.H. Ha, Biophys. Chem. 57 (1996) 155]. While at high pH and ionic strength, we found a similar behavior as reported earlier, at low ionic strength the light effect proved to be more complex. The main conclusions are the following: Though the number of BR excited to the photocycle (fraction cycling, fc) goes to saturation with increasing laser pulse energy, the absorbed energy by BR increases linearly with pulse energy. From the local analysis we conclude that the light effect changes the kinetics much earlier, already at the L intermediate state decay. The transient electric signal, caused by proton release and uptake, can be decomposed into two components similarly to the absorption kinetic data of the M intermediate state. The actinic light energy affects mainly the ratio of the two components and the proton movements inside BR while pH has an effect on the kinetics of the proton release and uptake groups at the membrane surface. 

*Keywords:* Bacteriorhodopsin; Proton pump; Actinic light effect; pH dependence

## 1. Introduction

The actinic light which excites the photocycle of bacteriorhodopsin (BR) has an interesting effect on the photocycle kinetics [1–5]. It was found that exciting the photocycle with a short laser pulse the amplitude of the slow component in the biphasic decay of the M intermediate state increases with increasing light intensity (pulse energy). It means that the excitation energy determines not only the cycling number (fraction cycling, fc) of BR but it has some nonlinear effect on the photocycle kinetics. Several mechanisms were proposed to explain this light intensity effect: directional cooperativity within a trimer [6], heterogeneity in BR population [4], protein structural changes that change some rate constants in the photocycle kinetics [5].

BR functions as a proton pump: during the photocycle, a proton is released and taken up by BR. One can assume that actinic light has an effect not only on the photocycle kinetics but on the proton pump

* Corresponding author. E-mail: pappe@ludens.elte.hu

0301-4622/98/$19.00 
*PII* S0301-4622(98)00102-1

too. Here, we report the results of the study of actinic light effect on the proton release and uptake during the photocycle. For the detection of proton release and uptake, an electrical method, worked out earlier [7,8], was applied. This method allows time resolution and kinetic study of the small conductivity change signal, caused by the transiently released protons during the photocycle, but presently this method can be applied only at low ionic strength. The pH dependence of the proton release kinetics was also studied. For comparison with photocycle kinetics and earlier results on cooperativity, absorption kinetic measurements were made at 410 nm and the data were analyzed within the local analysis of the M state kinetics [9]. We found that the electrical signal consists of two components, similarly to the fast and slow components of the M intermediate state absorption kinetics. Actinic light affects mainly the proton channels inside BR while the proton release and uptake by the membrane surface sites depend more strongly on pH.

## 2. Materials and methods

For detection of the small conductivity change during the photocycle, a bridge method was applied. The details of the method were given in Refs. [7,8]. The data were recorded by a digital storage adaptor (DSA-524, Thurlby-Thandard, England) and were stored in PC. For the excitation of the photocycle, a Nd-YAG laser (Quanta-Ray GCR-130, Spectra-Physics, USA), frequency doubled to 532 nm, was used (pulse duration ~ 7 ns). For the study of the actinic light effect, the starting laser pulse energy (approximately 20 mJ over 1 $cm^2$ laser beam, this corresponds later to A) was attenuated by neutral glass filters with attenuation of ~ 2.8, step by step (B, C, D, E).

The purple membrane (PM) suspensions isolated from *Halobacterium halobium* strain S9 were gifts from the Biophysics Institute, Biological Research Center, Szeged, Hungary. As the applied measuring method detects relative changes in the conductivity, all electrical measurements were made at relatively low ionic strength: PM in distilled water (pH ~ 7), addition of appropriate amount of NaOH (pH ~ 8.7) and HCl (pH ~ 4.2).

Fraction cycling was determined by the following relation: $fc = (A_{410}/A_{570})(\varepsilon_{BR}/\varepsilon_M)$, where $A_{570}$ is the measured absorption of the sample at 570 nm, $A_{410}$ is the amplitude of the fitted curve to the experimental data, $\varepsilon_{BR}$ and $\varepsilon_M$ are molar extinction coefficients for the BR and the M state, respectively, for which we take $\varepsilon_{BR}/\varepsilon_M = 2.1$.

## 3. Results

### 3.1. Absorption kinetic measurements

Absorption kinetic data recorded at 410 nm were analyzed within the local analysis of the M state fully given in [9]. This irreversible kinetic model assumes two parallel, isospectral M states ($M_1$ and $M_2$) with four rate constants ($k_1$, $k_2$ for buildup and $k_3$, $k_4$ for decay). The amplitudes of the two components ($M_1$ and $M_2$) are determined mainly by $k_1$ and $k_2$ (Eq. (22) in [9]):

$$a_1 = \frac{ak_1}{k_1 + k_2 - k_3}$$
$$a_2 = \frac{ak_2}{k_1 + k_2 - k_4} \qquad (1)$$

Fig. 1 shows the Arrhenius plot of the rate constants at two different actinic light intensities (A and D) at pH = 8.8 (phosphate buffer) and 100 mM NaCl

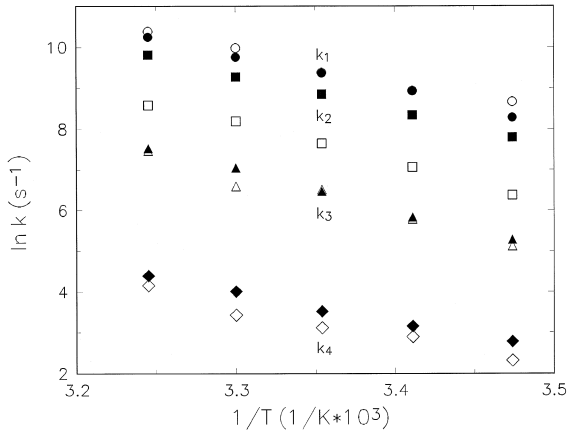


Fig. 1. Arrhenius plot of the rate constants at two exciting laser pulse energies. (Full symbols correspond to high (A), while open symbols to low (D) laser energies. pH = 8.8 (phosphate buffer) and 100 mM NaCl.)

concentration. As can be seen $k_1$ and $k_3$ do not change, $k_4$ changes (increases) slightly, but the main effect of increasing the actinic light intensity is the increase of the rate constant $k_2$. In the branching model, it leads to the increase of the amplitude of the slow decay component (Eq. (1)).

Fig. 2 shows the relative amplitude of the slow component ($a_2/a$) in dependence of the fraction cycling at different temperatures. This is a linear dependence, approximately independent of the temperature, with a slope of $\sim 0.7$ and with nonzero value at fc = 0.

Lowering the ionic strength (without salt and buffering), the kinetics and the actinic light effect change essentially. In general, at low ionic strength, the rate constants depend strongly on the actinic light intensity and they vary in a complicated way with the temperature and the actinic light intensity. Fig. 3 shows the relative amplitude of the slow component ($a_2/a$) in dependence of the fraction cycling at different temperatures and low ionic strength (pH ~ 7.3, PM in distilled water). Compared to Fig. 2, here, $a_2/a$ shows a strong temperature dependence, e.g., at 25°C, $a_2/a$ depends in an inverse way on fc (it decreases with increasing fc). The behavior at pH ~ 4.2 is similar, but with a smaller $a_2/a$.

### 3.2. Transient conductivity change measurements

The transient conductivity change, due to proton release and uptake during the photocycle, is detected

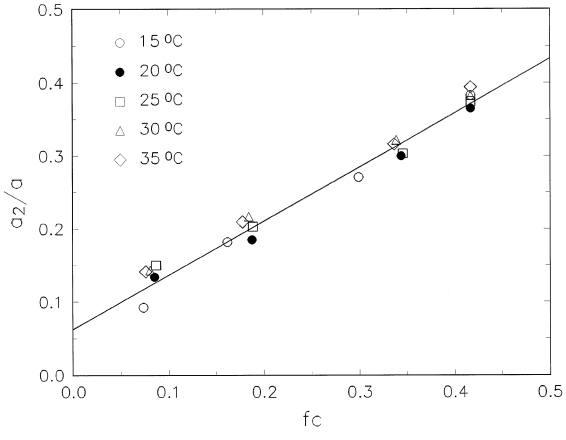


Fig. 2. The relative amplitude of the slow component in dependence of the fraction cycling (fc) for data partly presented in Fig. 1.

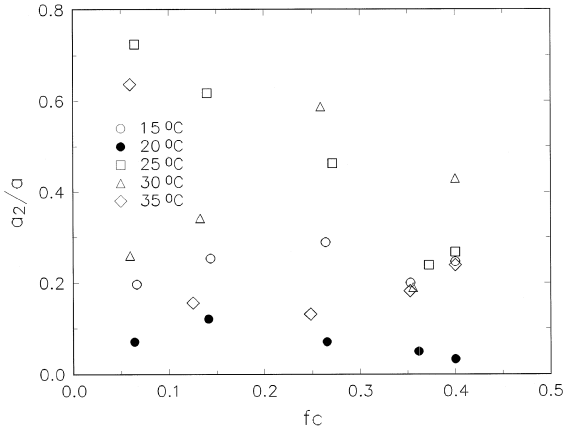


Fig. 3. The relative amplitude of the slow component in dependence of the fraction cycling at low ionic strength (PM in distilled water, pH ≈ 7.4).

as an unbalanced signal in the AC bridge (AC frequency 6 kHz), or as an amplitude modulation [7,8]. After demodulation [8], we get the time dependence of the transient conductivity change. Such signals are shown in Fig. 4A,E at two different exciting actinic light energies (PM in distilled water). Proton release corresponds to the increase, proton uptake to the decrease of the signal. Not only the amplitude of the signal (see later) depends on the actinic light energy but the time dependence too, in several ways. To analyze these changes, we used a curve-fitting program, described in Ref. [8] in more details. Here, we summarize the main points. The following function is fitted to the experimental data (Fig. 4A,E):

$$F(t) = a_1\{\exp[-k_2(t-t_2)] - \exp[-k_1(t-t_1)]\} + a_2\{\exp[-k_4(t-t_4)] - \exp[-k_3 \times (t-t_3)]\} + bt/t_0 + ct + const. \quad (2)$$

This function contains two components with different amplitudes ($a_1$ and $a_2$) and describes proton release and uptake at the membrane surface with rate constants $k_1,\ldots,k_4$ ($k_1$ and $k_3$ for release, $k_2$ and $k_4$ for uptake). $t_1,\ldots,t_4$ are time delays (relative to the exciting laser pulse), representing proton movements in the proton channels inside BR. The term with amplitude $b$ describes a laser pulse heating and it is proportional to the energy absorbed by BR

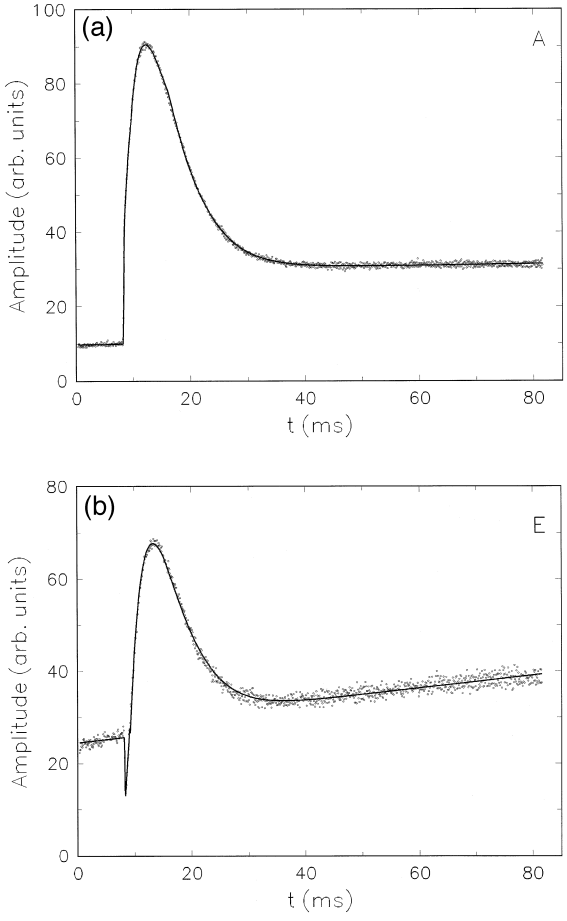


Fig. 4. Transient conductivity change after demodulation (scattered small circles) with decreasing (A and E) exciting laser pulse energies (PM in distilled water, 25°C). Solid line: a fit to Eq. (2).

during the excitation of the photocycle. The absorbed energy is given off to the surroundings within a time $t_0$ and causes a conductivity increase in the bulk. (The linear term, $ct$, represents the unbalanced difference between the two measuring cuvettes in the bridge. This unwanted effect is becoming more pronounced with decreasing laser excitation energy, see Fig. 4E, because the signal amplification is increased.) Eq. (2) fits (Fig. 4A,E solid lines) relatively well to the experimental points. In Eq. (2), there are 14 unknown parameters and some of them are strongly correlated (e.g., the amplitudes $a_1$ and $a_2$ strongly depend on the channel times $t_1,\ldots,t_4$), so their determination bears sometime large uncertainties.

The transient conductivity changes at low and high pH are shown in Figs. 5 and 6.

In the following, we summarize the behavior of the proton pump parameters in Eq. (2) in dependence of the actinic light energy and pH.

(1) The absorbed energy by BR during the laser excitation (determined from parameter $b$ in Eq. (2)) increases linearly with increasing laser pulse energy (Fig. 7). This is found at all pH. This observation is used to analyze the primary step in the photocycle and it is shown that the photo-equilibration between the BR-K states causes this linear increase.

(2) The amplitudes $a_1$ and $a_2$ in Eq. (2) are proportional to the number of pumped protons by BR's during the photocycle. It is interesting to compare the behavior of these amplitudes with the absorption kinetic data of the M intermediate state. We found a linear correlation at pH = 4.2 between the fraction cycling (fc, measured by absorption kinetic method at 410 nm) and the sum of the two amplitudes ($a = a_1 + a_2$). This is shown in Fig. 8. This reflects the expected result that the proton pump (quantum yield of proton release) goes to saturation with the exciting laser energy by the same way as the fraction cycling. Moreover, the amplitudes of the two components in proton release and in the absorption kinetic data are correlated too (Fig. 9). At higher pH values, the behavior of the amplitudes of the two components are similar, but the correlation is not so

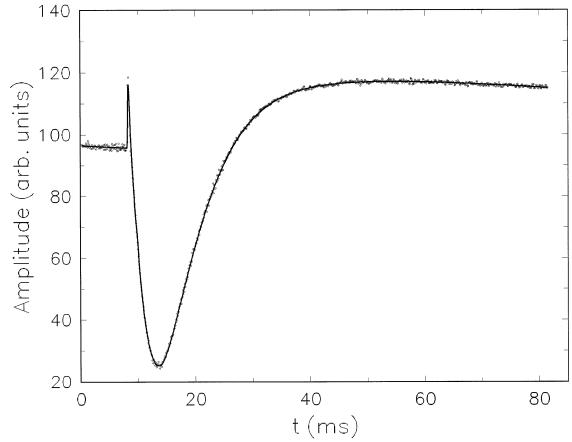


Fig. 5. Transient conductivity change (scattered small circles) at the high (A) laser pulse energy (pH = 4.2, temperature 25°C). Solid line: a fit to Eq. (2).

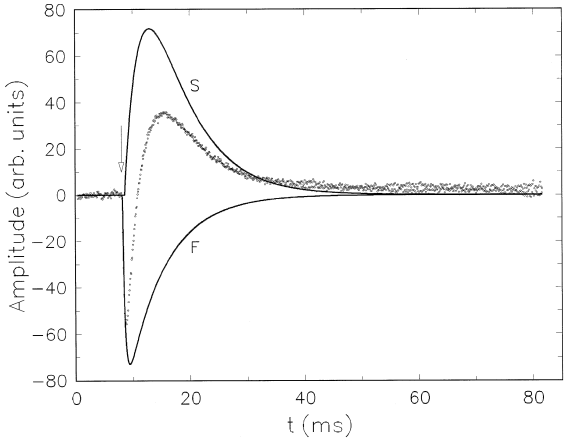


Fig. 6. The fast (F) and slow (S) components in proton release and uptake (solid lines) and the measured conductivity change (pH = 8.7, temperature 25°C). The small shift upward for the experimental points at longer times is the laser heating. The arrow shows the laser pulse (energy $E$).

clear. We attribute this distinction mainly to the uncertainties in the determination of the amplitudes when the channel times $t_1$, $t_2$ are nearly equal (see later).

(3) The relaxation time, $t_0$, for the laser pulse heating effect falls well within the photocycle ($\sim 9$ ms for data in Figs. 4 and 6). It decreases slightly at the lowest laser energy, but it is strongly temperature-dependent, similarly to the photocycle.

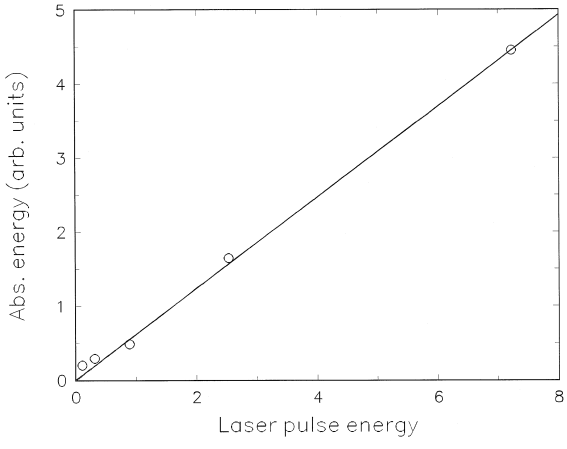


Fig. 7. The absorbed energy by BR (parameter $b$ in Eq. (2)) as a function of laser pulse energy for data partly presented in Fig. 4A and E. (Open circles are experimental data, solid line is a fit to Eq. (7).)

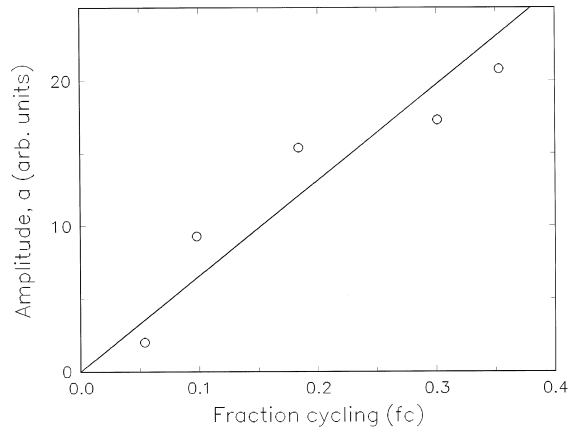


Fig. 8. Total amplitude ($a = a_1 + a_2$) of the electric signal as a function of the fraction cycling, measured by absorption kinetics at 410 nm (pH = 4.2, temperature 25°C).

(4) The electric signal (transient conductivity change) distinctly shows a time delay compared to the M intermediate state rise and decay, measured by absorption change at 410 nm. This delay is described by the channel times, $t_i$, in Eq. (2). A strong dependence of channel times $t_1$ and $t_2$ on the exciting laser pulse energy can be seen in Fig. 4A,E at pH = 7.4. As the laser pulse energy decreases, $t_1$ increases (from 0.14 to 0.32 ms) while $t_2$ decreases (from 0.49 to 0.17 ms). This leads to the appearance of a negative peak at the beginning of the electric signal (see Fig. 4E). It means that proton uptake

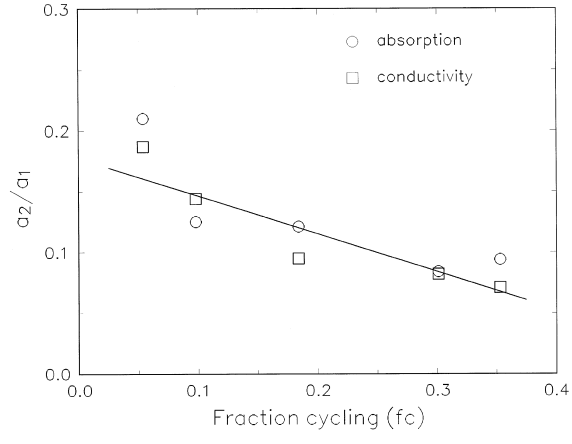


Fig. 9. The ratio of the amplitudes of the slow and fast components measured by absorption kinetics and by conductivity change as a function of the fraction cycling (pH = 4.2 and 25°C).

precedes proton release at lower laser energies at the PM surface. A similar effect is found at pH = 8.7 (see Fig. 6). At pH = 4.2, the channel times $t_1$ and $t_2$ are less sensitive to the laser pulse energy ($t_1 \approx 0.15$ ms and $t_2 \approx 0.24$ ms and here $t_1 < t_2$).

When the two channel times are nearly equal, the fitting leads to unrealistically high amplitude ($a_1$) values. The assumption, made in Eq. (2), that the channel times are well-defined values, is probably an oversimplification. More realistically, $t_1,\ldots,t_4$ follow a time distribution. The fitting program works better when the channel times are well separated (e.g., at pH = 4.2).

The determination of the channel times ($t_3$ and $t_4$) for the second, slow component in Eq. (2) is less certain. They are longer and fall in the ms range. (For pH = 7.4: $t_3 \sim t_4 \sim 1.2$ ms; for pH = 8.7: $t_3 \sim t_4 \sim 0.7$ ms and for pH = 4.2: $t_3 \sim 6$ ms and $t_4 \sim 2$ ms.) The channel times depend on the temperature too.

The electronic circuitry for measuring the electric signal contributes with a constant time delay to the channel times. This time delay is approximately 0.04 ms. It means that this method detects the appearance (or disappearance) of protons about 0.1 ms after the laser pulse.

(5) The rate constants ($k_1,\ldots,k_4$) for proton release and uptake at the membrane surface show a stronger pH dependence and less laser pulse energy dependence.

At pH = 7.4, the electric signal is mainly positive (Fig. 4A,E). This is because the rate constants for proton release are larger than the rate constants for uptake ($k_1,k_3 \sim 250\ s^{-1}$ and $k_2,k_4 \sim 220\ s^{-1}$).

At pH = 4.2, the electric signal is mainly negative (Fig. 5). Here, in the dominant fast component, $k_1 < k_2$. ($k_1 \sim 200\ s^{-1}$ and $k_2 \sim 300\ s^{-1}$. $k_2$ shows a stronger laser pulse energy dependence too.) This is the main reason for the well-known observation that at low pH, proton uptake is faster than proton release. The small positive peak at the start of the signal is caused by the shorter proton release channel time ($t_1 < t_2$). For the slow component, the rate constants have relatively low values ($k_3,k_4 \sim 25\ s^{-1}$).

At pH = 8.7, the electric signal has an unexpected complex time dependence (Fig. 6). In the fast component, proton uptake is faster than proton release, $k_2 > k_1$ and $k_2$ has a very high value ($k_1 \sim 150\ s^{-1}$ and $k_2 \sim 2500\ s^{-1}$). In the slow component, $k_3 > k_4$ ($k_3 \sim 250\ s^{-1}$, $k_4 \sim 170\ s^{-1}$) and this gives a positive peak later in the electric signal (Fig. 6). The two components in the fitting are also shown in Fig. 6.

## 4. Discussion

Exciting the BR with a short (~ 7 ns) laser pulse and increasing the pulse energy, the relative number of BR (fc) going to the photocycle first increases linearly (Fig. 10), but at higher pulse energies, it saturates at a level of FC ~ 0.4. (This saturation value which we denote by FC, shows a slight pH dependence, it increases with increasing pH.) From proton release and uptake measurements, we found (Fig. 7) that the energy absorbed by PM during one laser pulse increases approximately linearly with the laser pulse energy. To account for the saturation, one has to consider that the K intermediate state is a long-lived state (lifetime ~ $\mu$s) relative to the laser pulse length (7 ns) and there is a strong photoinduced back reaction K → BR. These two processes will determine the maximal number of BR cycling through the photocycle. (See also Ref. [10]. In our work, photoselection is not taken into account.) We can assume that during the excitation a BR molecule is either in the ground state (BR) or in the K

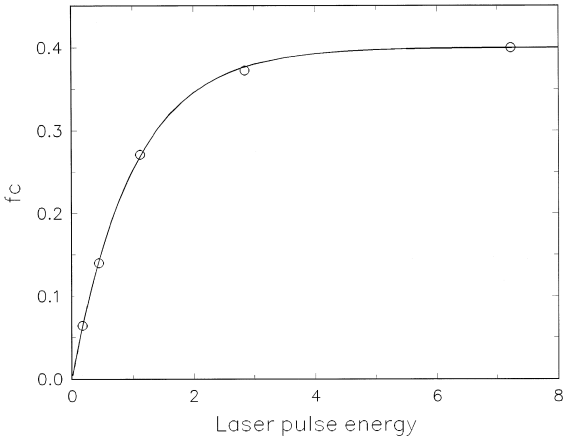


Fig. 10. The fraction cycling (fc) as a function of the laser pulse energy. (Circles are experimental values, line is a fit to Eq. (4)).

intermediate state. Then, the following differential equation can be written:

$$dn = b(N_0 - n)dt - cndt \quad (3)$$

Here, $N_0$ is the total number of BR molecules from which $n$ are in the K state at a given time, $t$, during the laser pulse. The first term in Eq. (3) gives the BR → K photoinduced transitions (through the BR* excited state and through J) and the second term gives the K → BR photoinduced back reaction. The constants $b$ and $c$ include the extinction coefficients ($\varepsilon_{BR}$, $\varepsilon_K$) of BR and K at the laser light wavelength, the quantum yield of the BR → K ($\Phi_{BR}$) and the K → BR ($\Phi_K$) transitions, and the laser light intensity. We take the following numerical values: $\Phi_{BR} = 0.64$ and $\Phi_K = 1$ [11,12]. Assuming a constant laser light intensity in the (0, $T$) time interval and zero outside (where $T \sim 7$ ns), Eq. (3) can be integrated giving the number of BR in the K intermediate state at the end of the laser excitation:

$$n = \frac{b}{b+c} N_0 [1 - e^{-(b+c)T}] \quad (4)$$

$n/N_0$ gives the fraction cycling at a given excitation energy. We can assume that all these BR in the K state ($n$) at the end of the photoexcitation will cycle through the photocycle [12]. The laser pulse energy is included in the exponent and thus the maximal fraction cycling is given by:

$$FC = \frac{n}{N_0} = \frac{b}{b+c} \quad (5)$$

The maximal fraction cycling is determined by the photo equilibration of BR and K, when in Eq. (4), $dn = 0$.

We have to emphasize that if the exciting light has a longer duration ($T \sim \tau_K$, where $\tau_K$ is the lifetime of the K state), then the decay of the K intermediate state to L has to be taken into account in Eq. (3). This will lead to a higher FC as it is found experimentally [3].

The absorbed energy by the BR molecules during the exciting light pulse is given by:

$$dE = \varepsilon a(N_0 - n)dt + \varepsilon cndt \quad (6)$$

where $\varepsilon$ is the exciting photon energy, $a$ and $c$ include only the extinction coefficients of BR and K ($\varepsilon_{BR}$, $\varepsilon_K$) and the exciting light intensity, so $b/a = \Phi_{BR}$. Integrating Eq. (6) by using Eq. (4), we get for the total absorbed energy during one laser pulse:

$$E = \varepsilon a N_0 T \left[1 - \frac{(a-c)b}{a(b+c)}\right] + \varepsilon N_0 \frac{a-c}{b+c} fc \quad (7)$$

For comparison with experiments, the experimental fc data were fitted to Eq. (4), taking the maximal laser pulse energy as 1 in the fit (Fig. 10). From the fit, we get the following numerical values for the parameters in Eq. (4): FC ≈ 0.4 and for the exponent $(b+c)T \approx 7.23$. As the exponent in Eq. (4) is proportional to the laser pulse energy, in the following, we take this value as the unit of the laser pulse energy. (It means that the applied 20 mJ maximal laser pulse energy corresponds to 7.23.)

The fit to Eq. (7) is shown in Fig. 7. As the measured absorbed energy is not calibrated, it was normalized to the theoretical value at the maximal pulse energy (at 7.23).

From Eq. (7), $E/\varepsilon N_0$ gives the average number of photons absorbed by a BR molecule. Dividing this value by fc (Eq. (4)), we get the average number of photons absorbed by a photocycling BR. This is shown in Fig. 11 with experimental data (circles) calculated from the measured fc and absorbed energy. Taking the reciprocal of the average number of photons, absorbed by a photocycling BR, we get the quantum efficiency of the photocycle. This is shown in Fig. 12. What is peculiar in the figure is that the

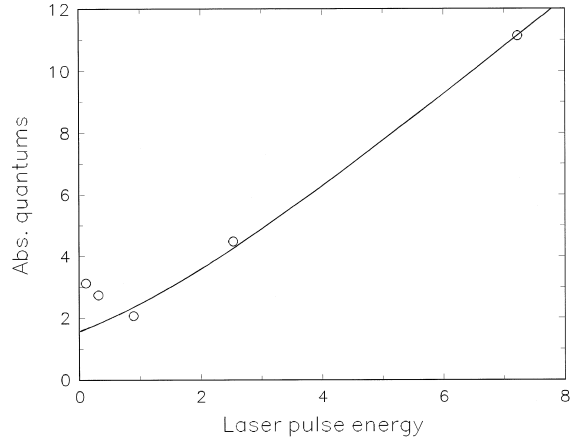


Fig. 11. Average number of photons absorbed by a photocycling BR in dependence of the laser pulse energy. (Circles are experimental values, line is derived from Eq. (7)).

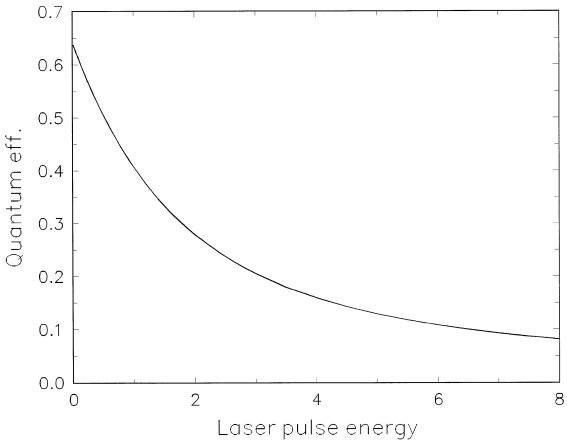


Fig. 12. Quantum efficiency of the photocycle as a function of the exciting laser pulse energy.

curve starts with a finite slope and the quantum efficiency drops suddenly with increasing pulse energy. To measure the starting value, one has to apply a very low exciting energy.

The effect of the exciting light intensity is a nonlinear effect in the sense that it leads to the change of the photocycle kinetics. This effect is most clearly seen at high pH and ionic strength as the relative increase of the slow component in the decay of the M intermediate state. No change was observed previously in the earlier part of the photocycle [2,5]. Several models have been proposed to explain the observed light effect [4]. The heterogeneity model assumes subpopulations in BR with different kinetics. The cooperative model takes into account direct or indirect interaction between photocycling BR in a given trimer (or between neighboring BR). Though a heterogeneous population of BR can not be excluded, in the following, we discuss only the cooperative model.

The simplest of this assumes [1] that if two or more BR are excited in the trimer, they all contribute to the slow component of the M decay. Tokaji [6] assumes a more specific interaction between photocycling BR in a trimer. This model gives a linear dependence on fraction cycling for the relative amplitude of the slow component in the M decay with a slope of 0.5.

The light effect was analyzed within a given (reversible) photocycle kinetics and it was concluded that protein structural changes at the cytoplasmic surface cause the cooperativity through the change of some rate constants in the late photocycle kinetics [5].

In this work, the light effect was analyzed within the local analysis [9] of the M state kinetics. This analysis uses only absorption kinetic data measured at 410 nm wavelength and assumes a branching around the L intermediate state. Within this model, the main effect of the exciting light is the increase of the $k_2$ rate constant with increasing laser pulse energy (Fig. 1). This leads to a temperature-independent linear relation between the relative amplitude ($a_2/a$) of the slow component and the fraction cycling (Fig. 2) at least at high pH and ionic strength. But this behavior is not general as decreasing the ionic strength (or changing pH) the light effect becomes more complicated and sensitive, e.g., to the temperature, and sometimes we observe a negative cooperativity, i.e., the slow component decreases with increasing exciting laser pulse energy (Fig. 9).

The essential difference in this analysis is the conclusion that the light effect causes changes in the photocycle kinetics much earlier, already at the decay of the L intermediate state. The results predicted by models based on direct interactions between photocycling BR [1,6] can be verified approximately only at specific conditions (high pH and ionic strength). (For example, we get a slope of 0.7 (Fig. 2) instead of the predicted 0.5 value [6].) We believe that a more general protein–protein interaction between photocycling BR can explain the complex light effect behavior. This interaction leads to the change in the photocycle kinetics and these changes are stronger or weaker at some points in the photocycle.

At low ionic strength, the charged groups at the PM surface are not shielded locally (the Debye length is large) and this can lead to an electric field inside the PM. This electric field can be partly the origin of the more complex light effect behavior at low ionic strength (Fig. 3).

The main effect of the exciting laser pulse energy on the proton pumping is twofold. It changes the relative amplitude of the slow component in proton release and uptake. A similar behavior is found in the M state kinetics, measured by absorption kinetic methods at 410 nm (Fig. 6). These effects must have

the same origin and they are connected to the deprotonation of the Schiff-base.

The laser pulse energy also has an effect on the channel times for the proton movement inside the PM. This is most pronounced at pH ≈ 7.4 (Fig. 4A and E) where it results in a negative peak in the early part of the electric signal. This effect support the idea of an indirect cooperative interaction: not only the retinal environment but the whole protein–retinal complex will be affected by the interaction.

The shortest channel time recorded by the electric method is ~100 μs (taking into account a ~40 μs electronic circuit delay in the electric signal). This is comparable with the time (70–80 μs) detected by pH-indicator dyes attached to some part of BR near to the membrane surface [13,14]. The channel times for the second component in the electric signal are much longer (~ms). This may be connected with different proton channels in BR for the two components.

The rate constants for proton release and uptake at the membrane surface mostly depend on the pH (and temperature). The exciting laser pulse energy has a less effect on these rate constants. A pronounced increase in the proton uptake rate constant ($k_2$) was observed at pH ≈ 8.7. It is not clear what could lead to this result.

The relaxation time, $t_0$, for the absorbed light energy release by PM falls within the decay of the M state. The introduced definite time, $t_0$, is an approximation. But it is known [15] from time-resolved photoacoustic measurements that BR releases most of the absorbed energy very early in the photocycle.

## 5. The main conclusions

Within the local analysis of the M state kinetics, the actinic light effect (cooperativity) leads to changes in the rate constants. The absorbed energy by BR increases linearly with the laser pulse energy though the fraction cycling goes to saturation. In proton release and uptake, there are two components (fast and slow) similarly to the M state kinetics and they are correlated. The light effect changes the ratio of the two components. The channel times also depend on the exciting laser pulse energy. The rate constants for proton release and uptake at the membrane surface mostly depend on the pH.

## Acknowledgements

We thank the Biophysics Institute of the Hungarian Academy of Sciences for providing PM preparations. This work was supported by the Hungarian Science Foundation grant 914 and FEFA.

## References

[1] K. Ohno, Y. Takeuchi, M. Yoshida, Photochem. Photobiol. 33 (1981) 573.
[2] Zs. Dancsházy, Zs. Tokaji, Biophys. J. 65 (1993) 823.
[3] A.Y. Komrakov, A.D. Kaulen, Biophys. Chem. 56 (1995) 113.
[4] R.I. Shrager, R.W. Hendler, S. Bose, Eur. J. Biochem. 229 (1995) 589.
[5] Gy. Váró, R. Needleman, J.K. Lanyi, Biophys. J. 70 (1996) 461.
[6] Zs. Tokaji, Biophys. J. 65 (1993) 1130.
[7] E. Papp, G. Fricsovszky, J. Photochem. Photobiol. B Biol. 5 (1990) 321.
[8] E. Papp, V.H. Ha, J. Photochem. Photobiol. B Biol. 29 (1995) 141.
[9] E. Papp, V.H. Ha, Biophys. Chem. 57 (1996) 155.
[10] J.F. Nagle, S.M. Bhattacharje, L.A. Parodi, R.H. Lozier, Photochem. Photobiol. 38 (1983) 331.
[11] J. Tittor, D. Oesterhelt, FEBS Lett. 263 (1990) 269.
[12] R. Govindjee, S.P. Balashov, T.G. Ebrey, Biophys. J. 58 (1990) 597.
[13] J. Heberle, N.A. Dencher, Proc. Natl. Acad. Sci. U.S.A. 89 (1992) 5996.
[14] U. Alexiev, R. Mollaaghababa, P. Sherrer, H.G. Khorana, M.P. Heyn, Proc. Natl. Acad. Sci. U.S.A. 92 (1995) 372.
[15] D. Zhang, D. Mauzerall, Biophys. J. 71 (1996) 381.